Optica Applicata, Vol. XXXVIII, No. 1, 2008

The effect of the size of the substrate grain made of submicrocrystalline sintered corundum on the bioglass composite structure and certain physico-mechanical properties of the bioglass

STANISŁAWA SZARSKA[1*], BARBARA STANIEWICZ-BRUDNIK[2], MAŁGORZATA LEKKA[3]

[1]Institute of Physics, Wrocław University of Technology, Wybrzeże Wyspiańskiego 27, 50-370 Wrocław, Poland

[2]Institute of Advanced Manufacturing Technology, ul. Wrocławska 37A, 30-011 Kraków, Poland

[3]Institute of Nuclear Physics PAN, ul. Radzikowskiego 152, 31-342 Kraków, Poland

[*]Corresponding author: Stanislawa.Szarska@pwr.wroc.pl

Advances in biomedical materials now make it possible to grow constructs outside the body and to use them for repairing tissues. The following properties of artificial bone replacement materials are important: the mechanical ones and the bioactivity. Composite materials are designed to provide a combination of good mechanical properties (corundum) and bioglass (bioactivity), which cannot be achieved with a single phase material. The influence of the mechanochemical treatment of microcrystalline sintered corundum (MCC) substrates on certain physico-mechanical properties of bioglass composites has been investigated. The composites consist of MCC and glass $CaO–P_2O_5–SiO_2$ system. The following methods are used: estimation of the MCC degree reduction size: grain size distribution; description of the morphology and biocomposites structure: SEM, AFM; description of certain physico--mechanical properties: adhesion force.

Keywords: bioglass, biocomposite, adhesion force.

1. Introduction

Advances in biomedical materials now make it possible to construct composite materials and to use them as engineered tissues for repairing or replacing diseased or damaged tissues. An important group of biomaterials are bioceramics, which can be broadly classified as bioinert, bioactive and resorbable, depending on the type of response in the body. The examples of a bioinert material is medical grade alumina. Alumina (Al_2O_3) is one of the compounds most often used to produce ceramic

biomedical products. It possesses one stable and many metastable phases [1]. Bioactive materials stimulate a biological response from the body such as bonding to tissue.

The sol–gel process has a number of application for the production of porous bioactive glasses and ceramics. This process involves the hydrolysis of silicon alkoxide in a solution to form a colloidal solution (sol) and the subsequent chemical polymerization of silica units to form gel. The gel is heat treated and during this process it dries and forms a glass or ceramic structure at temperatures much lower than those used in classical methods. If these materials have pores with diameters larger than 100 μm, bone ingrowths can occur, which anchor the bone to the material. In surface reactive materials (bioglasses), the materials attach directly by chemical bonding with the bone. The mechanism of bone bonding to bioactive materials is thought to be a result of forming the hydroxyapatite (HA) layer of the materials after their immersion in body fluid.

The main disadvantage of bioglasses is their low tensile modulus. The microstructure of the glass-ceramics materials, its properties and the processing routes used all are very strongly interrelated. In particular, porosity has a significant effect on elastic constants which decrease with increasing of pores content. Porosity is one of the most common defects in these materials, which also negatively affects their strength. The low fracture toughness of glasses is the greatest impediment to their broader use in load-bearing orthopedic applications in the human body. The incorporation of particles into glass matrices forming composite materials is a common method used to increase the toughness of brittle materials [2].

The composite materials contain the alumina grains which are reinforcing agents (to improve mechanical performance) and a bioglass matrix.

2. Results and disscussion

2.1. Reinforcement materials

Technologies offered by particular producers differ in the manner of producing Al_2O_3 sole and in the conditions of converting it into gel. The trade name of the product is Cubitron. Submicrocrystalline sintered corundum is aluminium oxide (α-Al_2O_3), which can be an implant core of the ultradispersive structure received as a result of transforming the aluminium oxide sole into gel which is then modified with magnesium oxide (MgO). This allows us to obtain a specific structure of sinter containing short Al_2O_3 needles, separated by $MgAl_2O_4$ micro-threads. Mechanochemical treatment of Cubitron was presented in detail in [3]. Submicrocrystalline sintered corundum grains were subject to mechanochemical treatment for 5, 10 and 15 hours. They were examined by determining their specific surface area (S_{BET}), analysing their phase and size compositions. The specific surface area (S_{BET}) grew up three times (from 3.17 to 10.95 m^2/g). The size composition revealed that the distribution of differences in percentage shares of particular fractions (from <20 μm to 0.3 μm) for 5-hour

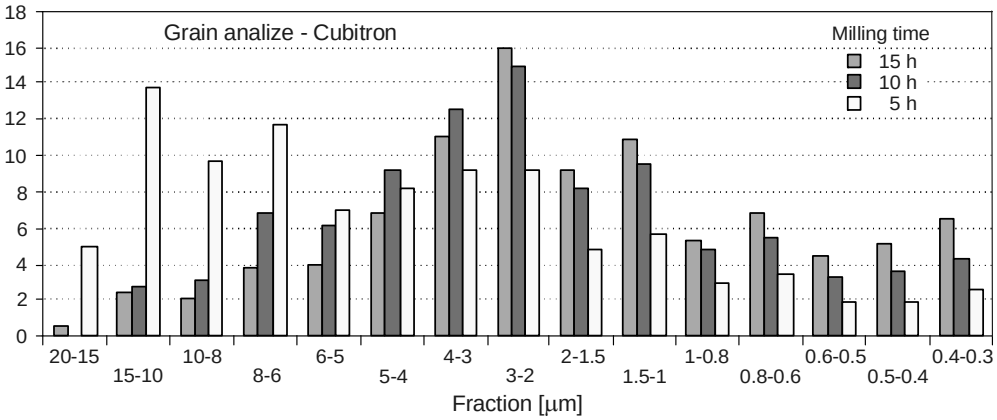

Fig. 1. Grain size analysis of milling Cubitron (submicrocrystalline sintered corundum).

milling gets the form of the *t*-Student distribution, and for 10- and 15-hour milling it is a classical Gaussian distribution.

The mean grain size of the cubitron surface is presented in Fig. 1.

2.2. Bioglass system

In agreement with earlier investigations [4, 5], the samples of biogel glasses with the nominal compositions 36CaO, 60SiO_2, 4P_2O_5 (mol%) were obtained. The basic composition of hydrolysate was prepared from the mixture of: tetraethoxysilane TEOS – $Si(OC_2H_5)_4$; calcium nitrate tetrahydrate $Ca(NO_3)_2 \cdot 4H_2O$ dissolved in distilled water; triethylphosphate $OP(C_2H_5O)_3$, ethanol C_2H_5OH as an organic solvent, 2N acid HNO_3 as a catalyst of the reaction of hydrolysis. The hydrolysates were mixed for about 2 hours.

Cubitron was added to the hydrolysate in a 1:0.028 ratio. The hydrolysate containing submicrocrystalline sintered corundum grains with input granulation corresponding to 5, 10 and 15 hours of milling, was left in ambient conditions to be gelled. The gelation which occurred in a range of 7 to 14 days, depending on the quantity of water used. Dried gels were subject to preliminary heat treatment at 60 °C (in a drier) for three days, and then hold in an electric furnace at 800 °C.

In Figure 2 the SEM (sintered corundum grains) and optical (biocomposite sample) images are presented.

Young's modulus *E* is also influenced by the microstructures, in particular by porosity and cavities. The value of *E* is also influenced by the presence of corundum grains dispersed randomly in the volume of the bioglass (depending on shape, size, concentration and *E* value of the dispersed particles, and especially on a mean degree of their aggregation or segregation). The microstructure is related to a corundum grains size, its distribution, and concentration of defects (pores, cavities, inclusions,

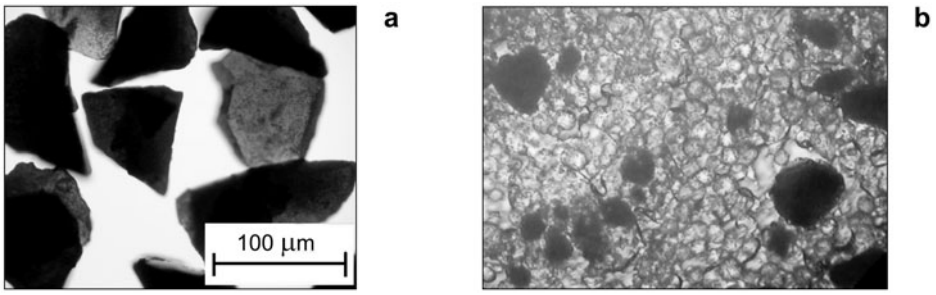

Fig. 2. SEM micrograph of unmilled Cubitron grains (**a**); optical microscope image of a biocomposite sample (**b**).

cracks). The grain boundary is a region where grains often join together and where the maximum concentration of defects appears. The mean grain size of the bioglass surface is measured by microphotography of a cross-section taken through an optical and AFM microscope equipped with a photocamera.

The biocomposite samples were immersed in a stimulated body fluid solution (SBF) at 37 °C and then examined under the AFM. We obtained two types of samples

T a b l e 1. Average height profile of the surface structure of bioglasses obtained by AFM topography.

Type of pore	Size [µm]	Deep [nm]
A	2.2	250
B	0.93	42
C	0.78	23
D	4.77	540
E	3.9	420
F	2.3	240
G	1.4	55

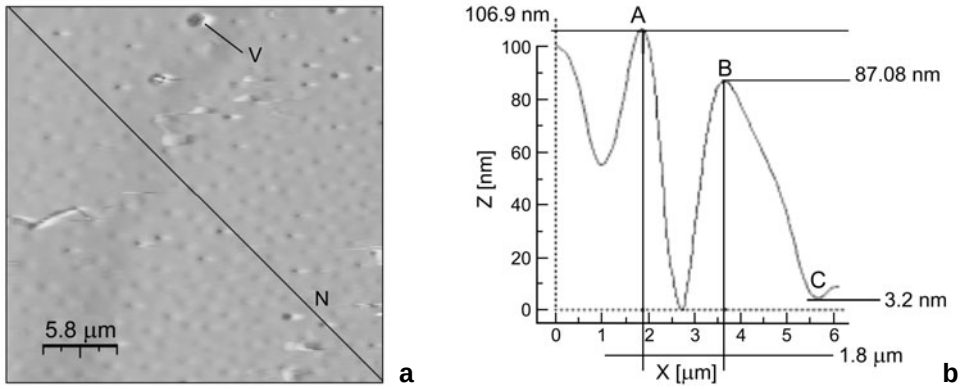

Fig. 3. AFM view of bioglass surface sample (**a**). Profile of V-pore before soking in SBF (**b**).

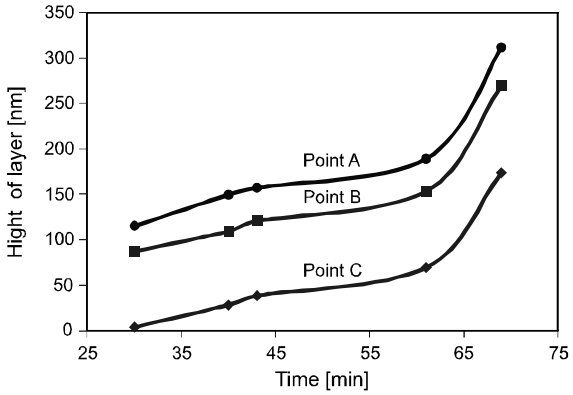

Fig. 4. Evolution of deep pore profiles as a function of bioglass surface immersion time in SBF.

with a bigger (*D*, *E*, *F*, *G*) and smaller (*A*, *B*, *C*) size of pores, depending on the water content.

Table 1 presents the average value of a size and height of investigated pores.

Figure 3 shows the characteristic pore V (*A*, *B*, *C* places) on which HA crystallite growth started.

Figure 3 presents the starting point of dynamic changes in the bioglass topography for 75 min of soaking in SBF. During the immersion of the sample in SBF, the increase of an apatite film on the pore sample (in *A*, *B*, *C* places) took place, which is presented in Fig. 4. The most conspicuous change of a pore profile was observed after 60–70 minutes of soaking in SBF. Its accretion was 14.2 nm per min.

3. Atomic force microscopy

A home-built atomic force microscope equipped with a liquid-cell setup was used [6]. Standard silicon nitride cantilevers (MLCT-AUHW type D, Veeco) were used as AFM probes with tip radii of about 50 nm. Their spring constants were monitored by resonant frequency of thermal excitations. The average value was 14.03 ± 2.1 kHz, respectively. Their similar values showed that used cantilevers had comparable mechanical properties. The determined, based on Sader's method [7], spring constant value was 0.0270 ± 0.0002 N/m.

The *force curves* reflecting the interaction between the modified AFM tip and the investigated surface were collected using the laser deflection technique. On each sample, 6 randomly chosen locations with the area of 10 and 30 μm^2 were measured. The number of curves recorded within the chosen area was 256 and 400, respectively.

The measurements were performed in a simulated body fluid (SBF solution) at room temperature. They were repeated three times with a newly coated cantilever.

The adhesion of Al_2O_3 coating to the bioglass surface was investigated by analyzing the single force curves (see Fig. 5). Then, the force histograms were

produced for each modified cantilever and for each sample. Next, the Gaussian distribution was fitted to the highest maximum. The center of the distribution corresponds to the most probable adhesion force, defined as a force needed for the separation of an AFM tip (modified with Al_2O_3) and the sample surface. The calculated

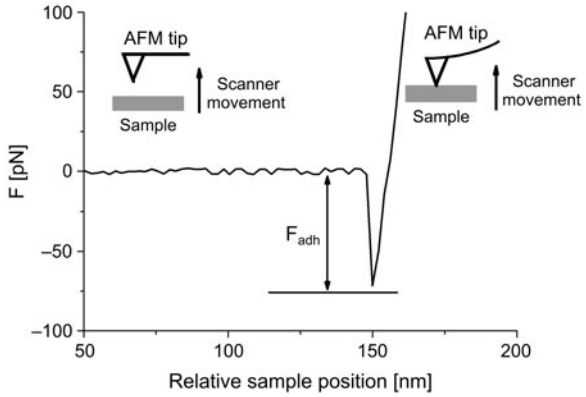

Fig. 5. The idea of the adhesion force determination. F_{adh} is determined as a difference between the free cantilever position (at $F = 0$) and the minimum value of the measured force.

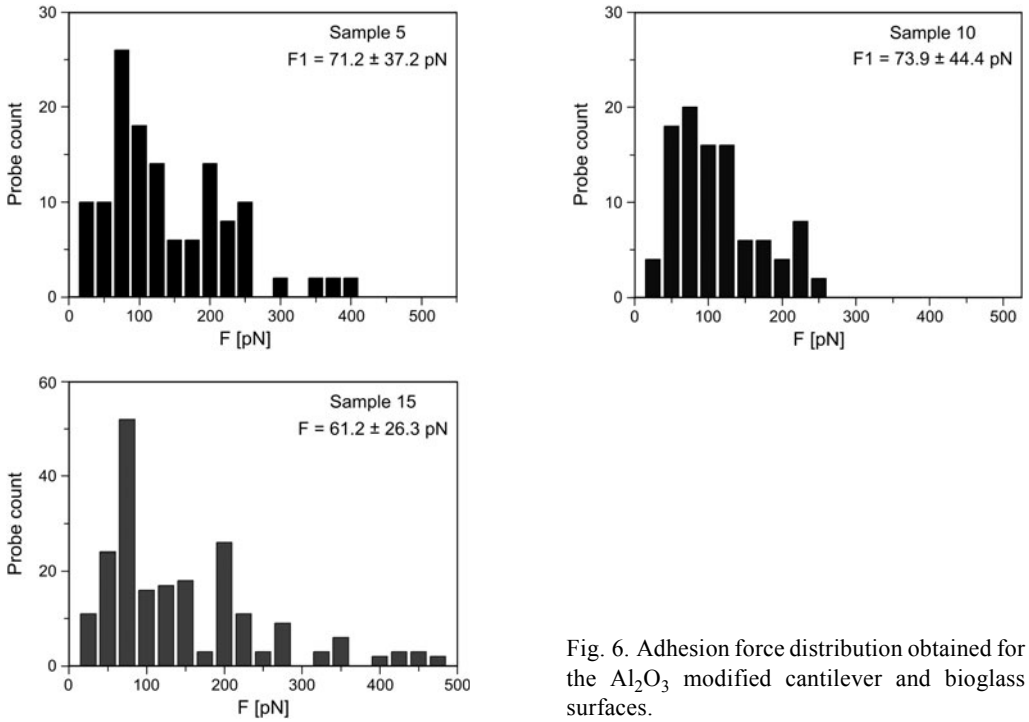

Fig. 6. Adhesion force distribution obtained for the Al_2O_3 modified cantilever and bioglass surfaces.

T a b l e 2. Parameters obtained from the AFM analysis.

	Cantilever #1	Cantilever #2	Cantilever #3
Unbinding force [pN]			
F_{adh} (sample p5)	63.2 ± 33.2	71.2 ± 37.2	75.21 ± 41.2
F_{adh} (sample p10)	55.9 ± 27.4	73.9 ± 44.4	70.4 ± 28.2
F_{adh} (sample p15)	71.3 ± 30.5	61.2 ± 26.3	69.8 ± 32.5
Unbinding probability [%]			
p_{unb} (sample p5)	8.7 ± 3.4%	4.7 ± 1.3%	19.4 ± 9.8%
p_{unb} (sample p10)	10.2 ± 5.6%	4.3 ± 2.3%	16.3 ± 4.6%
p_{unb} (sample p15)	15.1 ± 5.2%	10.4 ± 4.2%	22.2 ± 6.1%

standard errors were the measure of the uncertainity of the evaluation of the Gaussian distribution center.

The unbinding probability was defined as a ratio of the number of curves showing an adhesive event and the total number of recorded force curves. Its value was presented as a *mean* ± *standard deviation* and was calculated as a mean value for each studied case (for a particular cantilever and sample).

In Figure 6 the adhesion force distributions are shown for the cantilever modified with Al_2O_3 and three different surfaces denoted as p5, p10 and p15.

In all histograms, clearly one peak was observed at a position between 60 and 75 pN. It was fitted with the Gaussian function in order to estimate the most probable unbinding force. The obtained values are presented in Tab. 2.

The values of the most probable force needed to unbind the Al_2O_3 coated cantilever and the surface of bioglass were similar within experimental uncertainty, in all studied cases. This indicates that during the contact the same types of bonds are formed, and moreover, that the number of bonds within the contact area is comparable and independent of the chosen cantilever and sample measured. However, the character of these force histograms was rather not unimodal but it changed into asymmetric distributions showing sometimes bimodal character. The observed two maxima showed that the values of the adhesion force can be attributed to two most probable numbers of contact points located in the contact area between the tip and the investigated surface.

The unbinding probability can be attributed to the number of adhesive sites present on the surface. Therefore, its higher value can indicate the more adhesive properties of the surface, under the assumption that: *i*) all measurements were performed in randomly chosen locations on a sample surface, and *ii*) the surface properties were relatively homogenous. The studied samples p5, p10 and p15 were not completely heterogeneous, what was showed by large discrepancy of the unbinding probability value (see large values of the calculated standard deviation). For example, for the cantilever #2 and the sample p10, the unbinding probability values changed from

1.5% to 7.5%. Also, one can stress that in the case where only the adhesion force is delivered known and the exact contact area is not known, it is difficult to predict how many bonds were formed.

4. Conclusions

The applied technique of obtaining bioglass composites by immersing of the grains in the sol of $CaO–SiO_2–P_2O_5$ glass system, gelling and sintering in 800 °C allowed us to get gradient bioglass composites.

During the immersion of a sample in SBF, the growth of an apatite film on the pore sample took place, and the most changes of pore profiles were observed after 60–70 minutes.

The unbinding probability can be attributed to the number of adhesive sites present on the surface. Therefore, its higher value can indicate the more adhesive properties of the surface, under the assumption that *i*) all measurements were performed in randomly chosen locations on a sample surface, and *ii*) the surface properties were relatively homogenous.

References

[1] KRAJEWSKI A., RAVAGLIOLI A., *Bioceramics and biological glasses*, [In] *Integrated Biomaterials Science*, [Ed.] R. Barbucci, Kluwer Academic, New York 2002.

[2] HENCH L.L., JONES J.R., *Biomaterials, Artificial Organs and Tissue Engineering*, Woodhead Publishing Limited, Cambridge 2005.

[3] STANIEWICZ-BRUDNIK B., SZARSKA S., GAMRAT K., *The influence of mechanochemical treatment of substratem on the bioglass composite structure*, J. Materials Science, in press.

[4] PEREIRA, M.M., CLARK A.E., HENCH L.L., *Calcium phosphate formation on sol-gel-derived bioactive glasses in vitro*, Journal of Biomedical Materials Research **28**(6), 1994, pp. 693–8.

[5] JONES J.R, HENCH L.L., *Factors affecting the structure and properties of bioactive foam scaffolds for tissue engineering*, Journal of Biomedical Materials Research B: Applied Biomaterials **68B**(1), 2004, pp. 36–44.

[6] LEKKA M., LEKKI J., MARSZALEK M., GOLONKA P., STACHURA Z., CLEFF B., HRYNKIEWICZ A.Z., *Local elastic properties of cells studied by SFM*, Applied Surface Science **141**(3–4), 1999, pp. 345–9.

[7] SADER J.E., LARSON I., MULVANEY P., WHITE R.L., *Method for the calibration of atomic force microscope cantilevers*, Review of Scientific Instruments **66**(7), 1995, pp. 3789–98.

Received September 18, 2007